Available online at www.sciencedirect.com

ScienceDirect

Biochimica et Biophysica Acta 1757 (2006) 1582–1591

BIOCHIMICA ET BIOPHYSICA ACTA

BBA

www.elsevier.com/locate/bbabio

CO-dependent H_2 evolution by *Rhodospirillum rubrum*: Role of CODH:CooF complex

Steven W. Singer, Marissa B. Hirst, Paul W. Ludden *

Department of Plant and Microbial Biology, University of California-Berkeley, 111 Koshland Hall, Berkeley, CA 94720-3102, USA

Received 16 June 2006; received in revised form 29 September 2006; accepted 4 October 2006
Available online 14 October 2006

Abstract

Upon exposure to CO during anaerobic growth, the purple phototrophic bacterium *Rhodospirillum rubrum* expresses a CO-oxidizing H_2 evolving enzymatic system. The CO-oxidizing enzyme, carbon monoxide dehydrogenase (CODH), has been purified and extensively characterized. However the electron transfer pathway from CODH to the CO-induced hydrogenase that evolves H_2 is not well understood. CooF is an Fe–S protein that is the proposed mediator of electron transfer between CODH and the CO-induced hydrogenase. Here we present the spectroscopic and biochemical properties of the CODH:CooF complex. The characteristic EPR signals observed for CODH are largely insensitive to CooF complexation. Metal analysis and EPR spectroscopy show that CooF contains 2 Fe_4S_4 clusters. The observation of 2 Fe_4S_4 clusters for CooF contradicts the prediction of 4 Fe_4S_4 clusters based on analysis of the amino acid sequence of CooF and structural studies of CooF homologs. Comparison of *in vivo* and *in vitro* CO-dependent H_2 evolution indicates that ~90% of the activity is lost upon cell lysis. We propose that the loss of two labile Fe–S clusters from CooF during cell lysis may be responsible for the low *in vitro* CO-dependent H_2 evolution activity. During the course of these studies, a new assay for CODH:CooF was developed using membranes from an *R. rubrum* mutant that did not express CODH:CooF, but expressed high levels of the CO-induced hydrogenase. The assay revealed that the CO-induced hydrogenase requires the presence of CODH:CooF for optimal H_2 evolution activity.

Keywords: Carbon monoxide dehydrogenase; Hydrogen; EPR; Hydrogenase

1. Introduction

H_2 has intriguing potential as an environmentally benign, renewable source of energy to replace hydrocarbon-based fuels [1]. Industrial methods to produce H_2 are energy intensive and consume fossil fuels as energy sources [2]. Biological production of H_2 by microorganisms occurs under mild conditions and may provide an attractive method to produce H_2. Optimizing biological hydrogen production requires understanding the enzymatic pathways through which H_2 is formed on a molecular level [3].

The purple phototrophic bacterium *Rhodospirillum rubrum* is an excellent model organism for the study of biological hydrogen production because it evolves H_2 through multiple pathways: nitrogenase-mediated H_2 evolution, fermentation in the absence of light, and CO-dependent H_2 evolution [4]. CO-dependent H_2 evolution, also known as the biological water–gas shift reaction, is an exergonic process that allows *R. rubrum* to grow in the absence of light with CO as its sole energy source (Eq. (1)) [5].

$$CO + H_2O \rightleftharpoons CO_2 + H_2 (\Delta G^\circ = -20\,\mathrm{kJ/mol}) \quad (1)$$

The gene products of two operons, *cooFSCTJ* and *cooMLXUH*, referred to as the *coo* regulon, are required for CO-dependent growth (Fig. 1) [6]. The transcription of these genes is regulated by the gene product of *cooA*, which is a constitutively expressed CO-responsive transcriptional regulator [7]. The *cooFSCTJ* operon codes for the CO-oxidizing enzyme, carbon monoxide dehydrogenase (CooS), an Fe–S protein (CooF), and

Abbreviations: CODH, carbon monoxide dehydrogenase; ACS/CODH, acetyl Co-A synthase/carbon monoxide dehydrogenase; MV, methyl viologen; BV, benzyl viologen; DTH, sodium dithionite; EPR, electron paramagnetic resonance; MOPS, 3-N-(morpholino)propanesulfonic acid; BSA, bovine serum albumin

* Corresponding author. Tel.: +510 643 3940; fax: +510 642 4995.
E-mail address: pludden@nature.berkeley.edu (P.W. Ludden).

0005-2728/$ - see front matter © 2006 Elsevier B.V. All rights reserved.
doi:10.1016/j.bbabio.2006.10.003

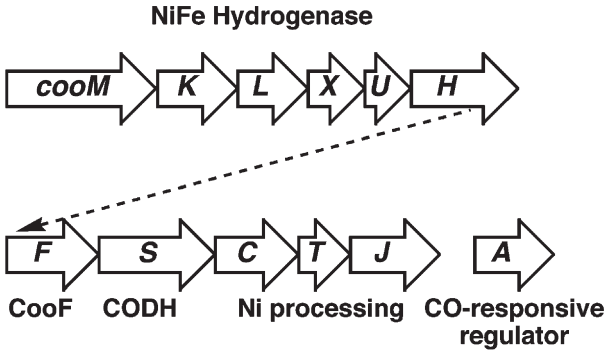

Fig. 1. Organization of the *coo* regulon. The *coo* regulon is divided up into gene clusters *cooMKLXUH* and *cooFSCTJ*, which are separated by a 450-bp region. The gene encoding for CO-responsive transcriptional regulator CooA is 137-bp downstream from *cooJ*.

gene products involved in Ni insertion into CooS (CooCTJ) [8]. The *cooMKLXUH* codes for a six-subunit [NiFe] hydrogenase that catalyzes H_2 evolution [9].

R. rubrum carbon monoxide dehydrogenase (CODH) is a membrane-associated protein that has been solubilized by heat treatment [10]. Structural studies revealed that *R. rubrum* CODH is an α_2 homodimer with five metal clusters [11]. Each subunit contains a $NiFe_4S_4$ cluster (C-cluster) and an Fe_4S_4 cluster (B-cluster). An Fe_4S_4 cluster (D-cluster) is located at the interface of the two subunits near the protein surface. Extensive evidence suggests CO oxidation occurs at the C-cluster and electrons travel through the B and D-cluster to external electron acceptors. The structure and arrangement of the metal clusters of *R. rubrum* CODH is nearly identical to CODH enzymes from hydrogenogenic bacterium *Carboxydothermus hydrogenoformans* and acetogen *Morella thermoacetica*. In *M. thermoacetica*, CODH is isolated in a protein complex with acetyl-CoA synthase (ACS/CODH) [12,13].

The CO-induced hydrogenase is a member of a class of membrane-bound multi-subunit [NiFe] hydrogenases referred to as Ech hydrogenases (*E*nergy *c*onverting *h*ydrogenase) [14]. Two subunits, CooH and CooL, are similar to the large and small subunits of standard [NiFe] hydrogenases involved in H_2 uptake. However, CooH and CooL have greater amino acid sequence similarity to subunits of NADH:quinone oxidoreductase (Complex 1), which conserves energy by proton translocation across the membrane during NADH oxidation. The four additional subunits of the CO-induced hydrogenase also have sequence similarity to subunits of Complex 1. Based on the analogy to Complex 1, it has been proposed that the CO-induced hydrogenase couples CO-dependent H_2 evolution to proton translocation, producing a proton gradient which drives ATP synthesis [15]. CO-dependent ATP synthesis has been demonstrated *in vivo* in the photosynthetic bacterium *Rubrivivax gelatinosa*, which possesses a CO-dependent H_2 evolution system very similar to *R. rubrum* [16]. Additionally, a ferredoxin-dependent Ech hydrogenase from *Pyrococcus furiosus* has been shown to couple H_2 evolution and ATP synthesis in inverted membrane vesicles [17].

CooF is a hydrophobic Fe–S protein that has sequence similarity to the electron transfer subunits of oxidoreductases such as *E. coli* nitrate reductase (NarH), *E. coli* DMSO reductase (DmsB), and *E. coli* formate dehydrogenase (Fdh-N β-subunit) [8]. The amino acid sequences of these proteins all contain cysteine-binding motifs for 4 Fe–S clusters. In the CO-dependent H_2 evolution system of *R. rubrum*, CooF links CO oxidation by CODH and H_2 evolution by the CO-induced hydrogenase [18]. When CO-grown *R. rubrum* membranes were treated with 20% ethanol, CODH was released from the membranes complexed to CooF. The CODH:CooF complex catalyzed methyl viologen (MV)-dependent CO oxidation at comparable rates to CODH purified by heat solubilization and had similar K_m values for CO and MV. CooF was required to reconstitute *in vitro* CO-dependent H_2 evolution using CODH: CooF-depleted *R. rubrum* membranes.

The biochemical characterization of CooF had several puzzling features. Though the amino acid sequence of CooF predicted binding sites for 4 Fe–S clusters, metal analysis of the purified protein obtained by Ensign and Ludden was consistent with the presence of only one Fe_4S_4 cluster. Also, the specific activity of reconstituted *in vitro* CO-dependent H_2 evolution ($\sim$0.1 μmol/min/mg protein) was much lower than would be expected based on measurements of *in vivo* CO-dependent H_2 evolution by *R. rubrum* ($\sim$1 μmol/min/mg protein) [19]. Recently, Hedderich and co-workers purified a CO-oxidizing/H_2 evolving complex from *C. hydrogenoformans*, a thermophilic eubacterium that utilizes CO as its sole carbon and energy source [20]. Biochemical and genetic analysis indicated that the subunit composition of the complex (CODH, CooF, CO-induced hydrogenase) was identical to the *R. rubrum* CO-oxidizing/H_2 evolving complex. Metal analysis of the complex was consistent with the presence of two CooF subunits in the complex and 4 Fe_4S_4 clusters in each CooF subunit.

The apparent discrepancies between the composition of CODH:CooF isolated from *R. rubrum* and *C. hydrogenoformans* prompted us to initiate a more detailed investigation of *R. rubrum* CODH:CooF and of *in vitro* CO-dependent H_2 evolution by *R. rubrum* membranes. A combination of spectroscopic and biochemical studies revealed that as-isolated *R. rubrum* CODH:CooF has only 2 Fe_4S_4 clusters and that the protein complex is unable to catalyze CO-dependent H_2 evolution at the levels observed *in vivo*. We propose that *in vivo*, CooF contains 4 Fe_4S_4 clusters, but two of the clusters may be labile and dissociate from the protein upon cell lysis. A new assay for CODH:CooF was developed using membranes from an *R. rubrum* mutant that did not express CODH:CooF, but expressed high levels of the CO-induced hydrogenase. The assay revealed that the CO-induced hydrogenase requires the presence of CODH:CooF for optimal H_2 evolution activity.

2. Materials and methods

2.1. Bacterial strains

R. rubrum strain UR2 is a spontaneous streptomycin-resistant mutant of *R. rubrum* ATC 11170 [21]. *R. rubrum* strain UR282 contains a kanamycin resistance cassette inserted into *cooF* that is polar onto *cooSCTJ* [8]. *R. rubrum*

strain UR294 contains a kanamycin resistance cassette inserted into *cooC* that is polar onto *cooTJ* [5].

2.2. Cell growth

R. rubrum strains were grown under photoheterotrophic conditions in 20 l polycarbonate carboys as previously described [22]. For Ni-depleted cultures, media were passed over a Chelex 100 resin before autoclaving. Cells were harvested by tangential flow filtration and stored under liquid nitrogen.

2.3. Enzyme purification

CODH:CooF was purified from CO-grown UR2 cells as previously described, except the preparative gel electrophoresis step was omitted [18]. Preparations of CODH:CooF were consistently 90–95% pure as determined by SDS-PAGE analysis and exhibited specific activities for CO-dependent methyl viologen (MV) reduction of 5000–6000 units/mg. CODH and CooF were separated by treatment with 30% acetonitrile as previously described. Both proteins were consistently >95% pure as determined by SDS-PAGE analysis and CODH exhibited CO oxidation activities of 5500–6000 units/mg. Ni-deficient CODH:CooF was purified with metal-free MOPS buffer and exhibited CO oxidation activities of 50–100 units/mg. Ni-deficient CODH and CooF were separated by 30% acetonitrile treatment and Ni-deficient CODH exhibited CO oxidation activities of 75–110 units/mg. Both Ni-deficient CODH:CooF and Ni-deficient CODH were activated ~25-fold in Ni insertion assays, performed as previously described [23].

2.4. Gel filtration

Analytical gel filtration experiments were performed on a 1.6×60 cm Superdex 200 column (Amersham Biosciences) equilibrated in 100 mM MOPS pH 7.5 containing 400 mM NaCl. Ferritin (440 kDa), catalase (232 kDa), aldolase (158 kDa), albumin (67 kDa) and ovalbumin (43 kDa) were employed for standardization of the column for molecular weight determination of CODH and CODH:CooF. Albumin (67 kDa), ovalbumin (43 kDa), chymotrypsinogen (25 kDa), and ribonuclease A (14 kDa) were employed for standardization of the column for molecular weight determination of CooF. The reported molecular weights of each protein are the average of two independent experiments.

2.5. EPR experiments

All gel filtrations were performed in a Coy anaerobic chamber (97% N_2, 3% H_2) with buffers that had been degassed and equilibrated with the chamber atmosphere for a week before use. A solution of CODH:CooF (6.5 mg/ml, 5700 units/mg) was desalted by gel filtration on G-25 Sephadex column (1.5×20 cm) in metal-free 100 mM MOPS buffer pH 7.5 to remove residual sodium dithionite (DTH). The desalted sample (~1.5 ml) was divided into 250 μl aliquots and placed into EPR tubes. The first sample was not treated, the second sample was treated with 50% reduced phenosafranin (λ_{max}=518 nm (oxidized), ε=25.7 mM^{-1} cm^{-1}) and the third sample was incubated with CO for 30 min. In another experiment, a solution of CODH:CooF (1.7 mg/ml, 5100 units/mg) was desalted by gel filtration on a G-25 Sephadex column (1.5×20 cm) and the resulting sample (~0.6 ml) was divided into 300 μl aliquots and placed in EPR tubes. One sample was treated with 4 mM DTH and the second sample was evacuated and then incubated with CO for 30 min, resulting in a solution under 100% CO. Samples of desalted CODH solutions (1.8 mg/ml, 5700 units/mg) were divided into 300 μl aliquots and reduced with 4 mM DTH and CO in an analogous manner for EPR analysis. Solutions of Ni-deficient CODH:CooF (8.5 mg/ml, 100 units/mg), Ni-deficient CODH (5.4 mg/ml, 110 units/mg) and CooF (0.69 mg/ml) were also desalted by gel filtration on a G-25 Sephadex column (1.5×20 cm) in metal-free 100 mM MOPS buffer pH 7.5 and reduced with 4 mM DTH. All samples reduced with DTH were incubated for 15 min before freezing in liquid nitrogen. X-band electron paramagnetic resonance spectra were recorded in the Spectroscopy Laboratory of the Advanced Light Source at Lawrence Berkeley National Laboratory. EPR was performed at a microwave frequency of 9.44 GHz and a modulation amplitude of 10 G using a Bruker ESP 300E EPR spectrometer equipped with a Bruker ER0815 frequency converter, a Bruker ER041 XG microwave bridge, and a Oxford ITC temperature controller. EPR spin quantitations were estimated with 1 mM CuEDTA as the standard.

2.6. Preparation of R. rubrum membrane suspensions

15 g of CO-grown UR2 cells were thawed in 50 ml of anaerobic 100 mM MOPS buffer pH 8.0 containing 1 mg DNase, 1 mg RNase, 20 mg lysozyme, 2 mM DTT, 4 mM DTH. Thawed cells were disrupted by French Press at 16,000 lb/in.^{2} under a stream of N_2, and unbroken cells were removed by centrifugation at 10,000×*g* for 10 min. Membranes were sedimented by centrifugation at 203,000×*g* for 2 h. The membranes were resuspended in 100 mM MOPS buffer pH 7.5 containing 2 mM DTH and pelleted into liquid nitrogen. For CO-grown UR282 cells, a membrane suspension was prepared by the same procedure from 18 g of cells thawed in 50 ml of buffer. For CO-grown UR294 cells, a membrane suspension was prepared from 20 g of cells thawed in 50 ml of buffer.

2.7. Comparison of CO-dependent H_2 evolution in R. rubrum whole cells and cell extracts

CO-grown UR2 cells (~0.5 mg) were thawed anaerobically and diluted in oxygen-free 100 mM MOPS pH 7.5 to a protein concentration of 39±3 mg/ml. The whole cell suspension (50 μl) was further diluted into 2 ml of 100 mM MOPS pH 7.5 containing 1 mM DTH and incubated under 13% CO; the gas phase (50 μl) was analyzed by gas chromatography. UR2 cell extract was prepared by thawing a portion of the same batch of CO-grown UR2 cells (20 g) in 100 mM MOPS pH 8.0 containing 1 mg DNase, 1 mg RNase, 20 mg lysozyme, 2 mM DTT, 4 mM DTH and breaking the cells by French press under a stream of N_2. The cell extract was centrifuged for at 10,000×*g* for 10 min to remove unbroken cells and the cell extract assayed for CO-dependent H_2 evolution activity as described below. Additional UR2 cell extracts were prepared by thawing a portion of the same batch of CO-grown cells (5 g) and breaking the cells by osmotic shock in a Coy anaerobic chamber [24].

2.8. Protein assays and metal analysis

SDS-PAGE was performed according to Laemmli [25]. Polyclonal anti-CooH antibodies were raised in rabbits at the Polyclonal Antibody Service of the University of Wisconsin-Madison [15]. Anti-CooH antibodies were treated with an acetone powder derived from UR2 membranes isolated from cells grown in the absence of CO to remove non-specific binding. Western blots were performed as previously described [26]. Protein concentrations were determined by the bicinchonic acid method using bovine serum albumin (BSA) as a standard [27]. Each protein determination is an average of three replicate assays. Protein metal content was determined by inductively coupled plasma mass spectrometry (ICP-MS) at the University of Georgia Chemical Analysis Laboratory. Metal analyses were performed on 3 independent preparations of CODH:CooF and CooF.

2.9. Activity assays

CODH activity was determined spectrophotometrically at A_{578} by the CO-dependent reduction of MV [21]. MV-dependent H_2 evolution was measured by gas chromatography with 2 mM MV and 40 mM DTH as previously described [18]. CO-dependent H_2 evolution was measured by gas chromatography with 13% CO and 1 mM DTH as previously described [18]. Three replicates of each assay were performed.

3. Results

3.1. Subunit composition and metal analysis of CODH:CooF and CooF

CODH:CooF from *R. rubrum* was previously reported to be a heterodimer, however, this assignment was incompatible with

the crystal structure of CODH, which shows CODH is a homodimer [11,18]. Gel filtration experiments were undertaken to determine the molecular weight of CODH:CooF, using CODH (~123 kDa predicted molecular weight for a homodimer) as a control. CODH eluted at an apparent molecular weight of 127 kDa on a HiLoad Superdex 200 prep grade column. CODH:CooF (167 kDa predicted molecular weight for a heterotetramer) eluted at an apparent molecular weight of 173 kDa and CooF (21 kDa predicted molecular weight for a monomer) eluted at an apparent molecular weight of 29 kDa.

In the original characterization of CODH:CooF, the metal content of CODH:CooF was estimated to be 1 Ni and 14 Fe/CODH:CooF heterodimer and 4 Fe/CooF monomer [18]. Metal analysis conducted on recent preparations of CODH:CooF estimated that CODH:CooF contained 1.8±0.1 Ni and 28±2 Fe/tetramer and CooF contained 7±2 Fe/monomer. Therefore, the metal analysis for CODH:CooF was essentially identical to the original report, while the metal analysis for CooF was different.

3.2. EPR analysis of CODH:CooF

CODH has been extensively characterized by EPR spectroscopy and this technique provides a convenient method to assess whether the metal clusters of CODH are altered by CooF complexation. The C-cluster has four discrete electronic states: C_{ox}, C_{red1}, C_{int}, C_{red2}. C_{ox} (EPR silent) is observed when CODH is poised at ~0 mV, C_{red1} is observed at intermediate potential ($E°=-110$ mV, $g_{avg}=1.87$), C_{int} (EPR silent) is observed when the solution potential is <−350 mV, and C_{red2} ($g_{avg}=1.86$) is observed when CODH is treated with CO or DTH [28,29]. The B-cluster has two states: B_{ox} (EPR silent) and B_{red} ($g_{avg}=1.94$, $E°=-418$ mV) [30]. An EPR signal for the D-cluster has not been observed [31].

As-isolated CODH:CooF was EPR silent, indicating the C-cluster was in the C_{ox} state and the B-cluster was in the B_{ox} state (Fig. 2). CODH:CooF poised with 50% reduced phenosafranin exhibited a rhombic spectrum at almost the same g values as the C_{red1} signal of CODH ($g=2.03$, 1.88, 1.72). The spin concentration measured for the C_{red1} state of CODH:CooF (~0.2 spins/tetramer) was similar to the results obtained for spin integration of the C_{red1} state of heat-solubilized CODH [32]. Upon incubation of as-isolated CODH:CooF with CO, a complex pattern of overlapping signals was observed in the EPR spectrum of the sample. Two of signals ($g=2.04$, 1.94, 1.89) and ($g=1.97$, 1.87, 1.76) had identical g values to B_{red} and C_{red2} signals observed for CO-reduced CODH. Only the $g=1.76$ feature of C_{red2} is observed, the other component are inferred based on EPR spectra of CODH. Also evident in the spectra of CO-reduced CODH:CooF was a prominent shoulder at $g=2.10$, most prominently in Fig. 3A at 4.5 K. The shoulder at $g=2.10$ has been observed in previous EPR studies of CODH and has been attributed to spin–spin coupling between the B-cluster and C-cluster of CODH [29]. The peak of a third, broad signal was observed at $g=2.01$; this signal is not observed in CO-reduced CODH. A study of the temperature dependence of the EPR

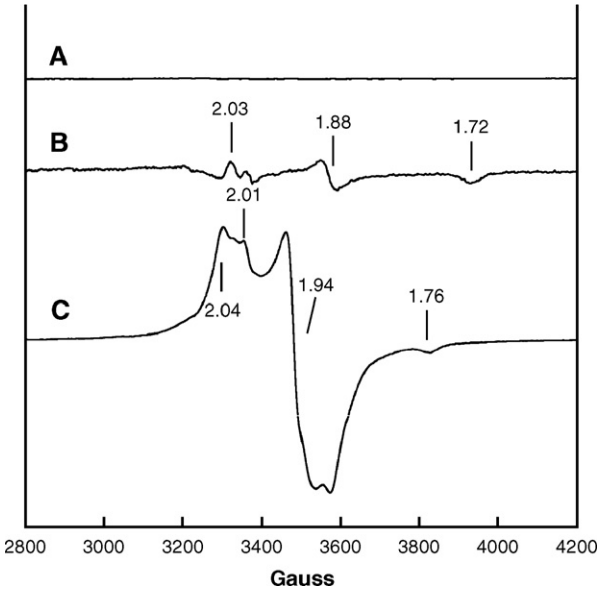

Fig. 2. EPR spectra of CODH:CooF. Spectrometer conditions were: microwave power, 10 mW; modulation amplitude, 10 G; frequency, 9.44 GHz; temperature, 10 K. Spectra shown were recorded for the following samples: A, As-isolated CODH:CooF; B, CODH:CooF poised with reduced phenosafranin; C, CO-reduced CODH:CooF.

spectrum of CO-reduced CODH:CooF showed that all the signals were maximized at 4.5 K and the C_{red2} signal was absent at 20 K (Fig. 3A). Integration of the CO-reduced spectrum relative to a Cu(II) EDTA standard obtained at 10 K and 1 mW power indicated the complex contained 6.5 spins/tetramer. The EPR spectrum at 10 K of CODH:CooF reduced with 4 mM DTH had a lower spin concentration than CO-reduced CODH:CooF (3.0 spins/tetramer) and lacked the C_{red2} signal (Fig. 3B). At 4.5 K, the C_{red2} signal was observed for DTH-reduced CODH:CooF, indicating DTH-reduced CODH:CooF has an altered temperature dependence compared to CO-reduced CODH:CooF. In contrast, the EPR spectrum of CO-reduced and DTH-reduced CODH obtained by acetonitrile treatment of CODH:CooF showed similar temperature-dependences and spin concentrations (CO-reduced CODH-2.6 spins/dimer; DTH-reduced CODH-2.8 spins/dimer at 10 K and 1 mW power) (data not shown).

3.3. EPR analysis of Ni-deficient CODH:CooF

The EPR spectrum of Ni-deficient CODH is simpler than that of Ni-CODH because it lacks the characteristic C-cluster signals present in the EPR spectrum of CODH [28]. Ni-deficient CODH:CooF was purified under the same conditions as CODH:CooF and Ni-deficient CODH was obtained by acetonitrile separation of Ni-deficient CODH:CooF. Both Ni-deficient CODH and Ni-deficient CODH:CooF were EPR silent at potentials >−400 mV (data not shown). The EPR spectrum of DTH-reduced Ni-deficient CODH at 10 K was nearly identical to previously published spectra, lacking any signals assigned to the C-cluster (Fig. 4A). Comparison of this spectrum with the EPR spectrum of DTH-reduced Ni-deficient CODH:CooF at

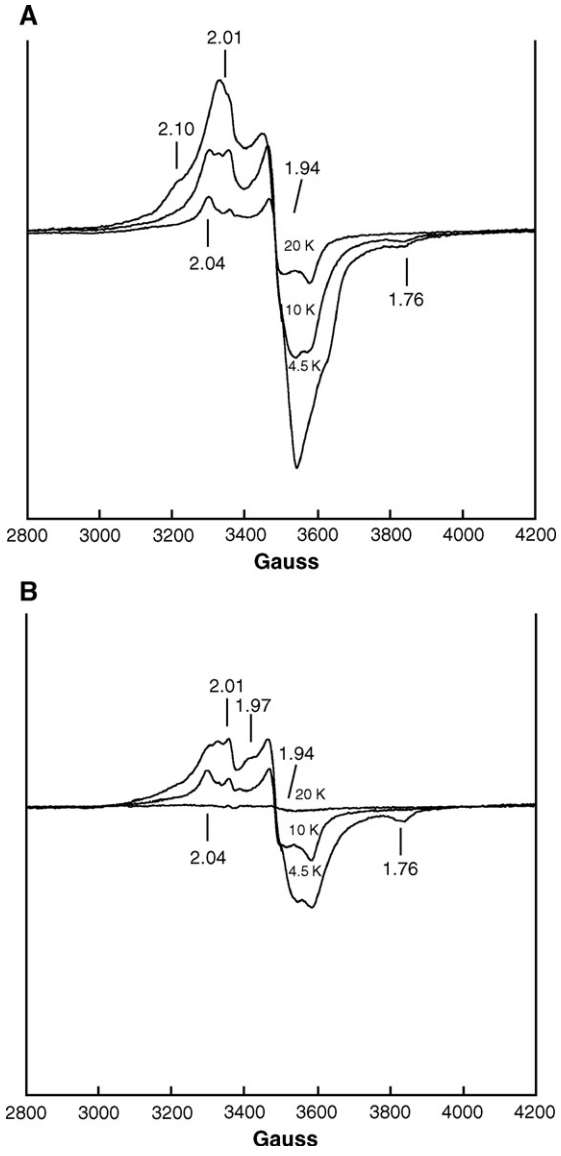

Fig. 3. Temperature dependent EPR spectra of reduced CODH:CooF. Spectrometer conditions were: microwave power, 10 mW; modulation amplitude, 10 G; frequency, 9.44 GHz; temperature, 4.5 K, 10 K, 20 K. Spectra shown were recorded for the following samples: A, CO-reduced CODH:CooF; B, DTH-reduced CODH:CooF.

10 K indicated that the spectra had the same features except for a broad signal with a peak at $g=2.01$ (Fig. 4B).

3.4. EPR analysis of CooF

The ability to separate CODH and CooF allowed the assignment of the EPR spectral features of CODH:CooF arising from CooF alone. When the EPR spectrum of DTH-reduced CooF was measured at 10 K, a broad signal centered at $g=1.94$

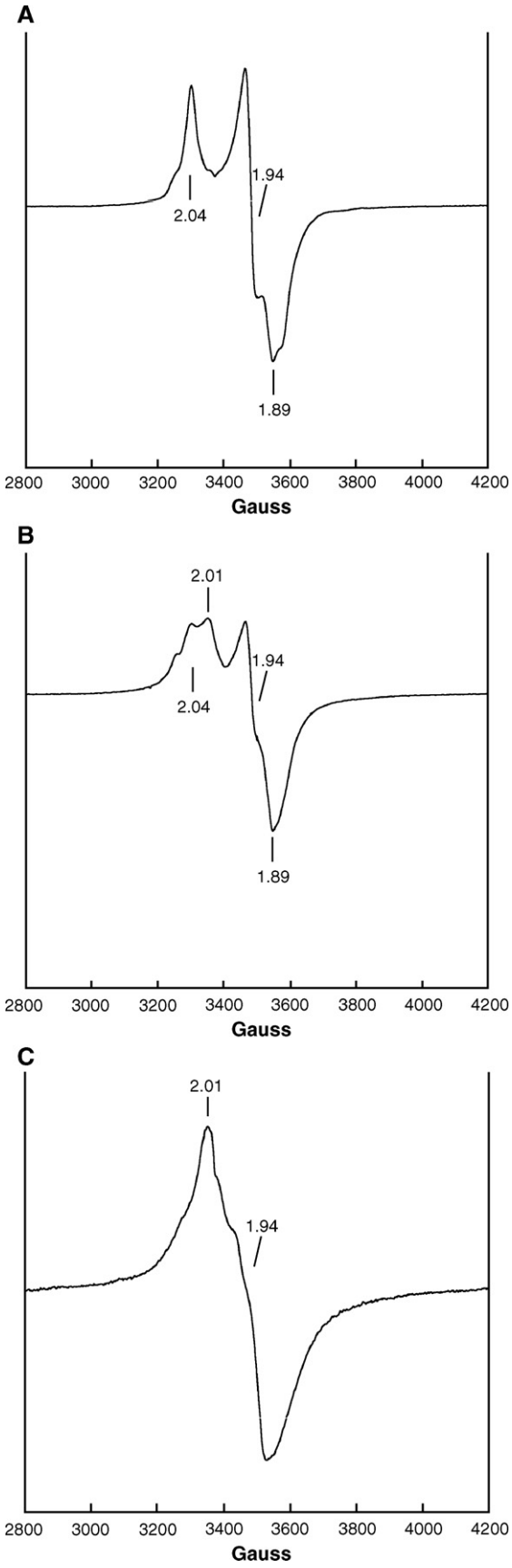

Fig. 4. Comparison of EPR spectra for Ni-deficient CODH, Ni-deficient CODH:CooF and CooF. Spectrometer conditions were: microwave power, 10 mW; modulation amplitude, 10 G; frequency, 9.44 GHz; temperature, 10 K. Spectra shown were recorded for samples: A, DTH-reduced Ni-deficient CODH; B, DTH-reduced Ni-deficient CODH:CooF; C, DTH-reduced CooF.

Table 1
Comparison of CO-dependent H_2 evolution by *R. rubrum* whole cells and cell extracts from CO-grown UR2

UR2 preparation	CO-dependent MV reduction (μmol/min/mg protein)	MV-dependent H_2 evolution (nmol/min/mg protein)	CO-dependent H_2 evolution (nmol/min/mg protein)
Whole cells	ND [a]	ND	580±80
Cell extract (French press)	39±3	390±40	34±4
Cell extract (osmotic shock)	30±5	740±50	60±8

[a] Not determined.

was observed (Fig. 4C). This signal corresponded to the unassigned signals observed in the spectra of CODH:CooF and Ni-deficient CODH:CooF. Integration of the spectrum of DTH-reduced CooF obtained at 10 K and 1 mW power relative to a Cu(II) EDTA standard indicated the protein had 2.0 spins/monomer. The spin integration of the CooF spectrum was consistent with the presence of two CooF monomers in the CODH:CooF complex, because ~4 additional spins were measured compared to spin integration of CODH. The EPR spectrum of DTH-reduced CooF probably arises from a magnetic exchange interaction of two $[Fe_4S_4]^{1+}$ clusters that are in close proximity in the protein [33]. Neither temperature nor power variation showed any resolution of the spectrum into individual $[Fe_4S_4]$ cluster signals (data not shown). This type of spectrum has often been observed in EPR studies of 8-Fe ferredoxins [34].

3.5. CO-dependent H_2 evolution activity is lost upon cell breakage

As mentioned in the Introduction, reported rates of *in vitro* reconstitution of CO-dependent H_2 evolution were ~10-fold less than the rates measured *in vivo* [19]. The observation of only two Fe_4S_4 in CooF led us to question whether the loss of activity was caused by damage to CODH:CooF. Initially, we considered the possibility that 20% ethanol treatment of CODH:CooF had damaged the complex and lowered the rate of *in vitro* CO-dependent H_2 evolution. However, both as-isolated UR2 membranes and CHAPS-washed membrane suspensions incubated with purified CODH:CooF had similar rates of CO-dependent H_2 evolution activity (~80 nmol/min/mg protein). Also, no substantial loss of activity was observed when *R. rubrum* cell extracts and membranes were compared, indicating that no components critical for CO-dependent H_2 evolution were removed when the soluble fraction and the membrane fraction were separated (Table 1). However, when CO-dependent H_2 evolution by *R. rubrum* whole cells was compared to cell extracts, which contain both the soluble and membrane fractions, after lysis by French press, a 17-fold loss of activity was observed. Similar losses in activity were observed when *R. rubrum* cells were lysed by osmotic shock, which is a milder cell lysis procedure than French press.

3.6. An improved assay for CODH:CooF

As a complement to spectroscopic studies of CODH:CooF, we initiated development of an alternative biochemical assay for CODH:CooF to understand more completely electron transfer through the protein complex. The CO-dependent MV reduction is the standard assay for CODH activity. Both CODH and CODH:CooF have similar activities in the MV assay, so the activity of CooF cannot be directly assayed by this method. CO-dependent reduction assays were developed with other electron-accepting dyes (methylene blue, 2-hydroxy-1,4-napthoquinone, phenosafranin), however all dyes tested showed similar levels of activity for CODH and CODH:CooF (data not shown). Ensign and Ludden developed an assay for CODH:CooF based on reconstitution of CO-dependent H_2 evolution with *R. rubrum* membranes selectively depleted of CODH:CooF by detergent wash [18]. This assay had the advantage of reproducing the activity observed under physiological conditions. However, this assay required repeated washing of the membranes and components critical to fully reconstituting CO-dependent H_2 evolution may have been lost. A new assay was developed using membranes obtained from CO-grown cells of UR282, an *R. rubrum* strain with kanamycin cassette inserted into *cooF* that is polar onto *cooSCTJ* [8]. UR282 membranes were essentially inactive in CO-dependent MV-reduction or CO-dependent H_2 evolution but exhibited significant MV-dependent H_2 evolution activity (Table 2). Upon addition of purified CODH:CooF to a UR282 membrane preparation, CO-dependent H_2 evolution activity was observed; no activity was observed when purified CODH was added (data not shown).

Comparison of intact (CODH:CooF-containing) UR2 membranes and reconstituted UR282 membranes indicated that both CO-dependent and MV-dependent H_2 evolution were higher in UR2 membranes (Table 2). Previous studies have indicated that the two other hydrogenases expressed by *R. rubrum*, an uptake hydrogenase and a formate-induced hydrogenase, are present at very low levels in *R. rubrum* cells grown in the presence of CO and malate [4,15,35]. Therefore H_2 evolution by the *R. rubrum* membranes may be attributed to the activity of the CO-induced hydrogenase. This surprising difference was initially attributed to a decreased level of expression of the subunits of the CO-

Table 2
Comparison of *in vitro* CO-dependent H_2 evolution by *R. rubrum* membranes of CO-grown cells of UR2, UR282 and UR294

Strain [a]	CO-dependent MV reduction (μmol/min/mg protein)	MV-dependent H_2 evolution (nmol/min/mg protein)	CO-dependent H_2 evolution (nmol/min/mg protein)	CO-dependent H_2 evolution with added CODH:CooF [b]
UR2	61±6	840±70	72±6	75±5
UR282	<0.01	290±20	<0.1	27±6
UR294	3.0±0.1	1200±60	26±1 [c]	28±4

[a] Concentrations of *R. rubrum* membranes: UR2, 30±3 mg/ml; UR282, 29±2 mg/ml; UR294, 23±1 mg/ml.
[b] 150 μg of CODH:CooF (1.7 mg/ml, 5100 units/mg) was added to membrane preparations.
[c] Whole cell CO-dependent H_2 evolution activity for UR294 was 180±10 nmol/min/mg protein.

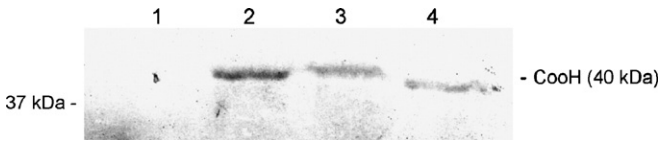

Fig. 5. Western blot analysis of membrane fractions of UR2, UR282 and UR294 developed with antibodies to CooH (1:750 dilution). Lane 1, membranes from uninduced UR2 cells (105 μg protein); lane 2, membranes from CO-grown UR282 cells (87 μg protein); lane 3, membranes from CO-grown UR294 cells (92 μg protein); lane 4, membranes from CO-grown UR2 cells (90 μg protein). Ponceau staining indicated that similar levels of protein were present in the four membrane preparations (data not shown).

induced hydrogenase. However, Western blot analysis of UR2 and UR282 using antibodies raised against CooH, the catalytic subunit of the CO-induced hydrogenase, revealed a 2.5-fold higher level of CooH expression in UR282 membranes compared to UR2 membranes (Fig. 5, Lane 2 and Lane 4). Taking into account H_2 evolution activity and CooH expression, UR2 membranes were 7.5-fold more active than UR282 membranes. In comparison, membranes of UR294, an *R. rubrum* mutant that has a kanamycin cassette inserted into *cooC* that is polar on to *cooTJ*, exhibited H_2 evolution activities that were comparable to UR2 membranes, when corrected for the increased amount of CooH in UR294 membranes (1.5-fold greater than UR2 membranes) (Fig. 5, Lane 3).

4. Discussion

4.1. Characterization of CODH:CooF

The initial objective of this work was to characterize CODH:CooF in detail to determine the effect of CooF complexation on the properties of the metal clusters of CODH. The native molecular weight of CODH:CooF was estimated to be 173 kDa by analytical gel filtration chromatography, establishing that the complex has an $\alpha_2\beta_2$ structure with a dimeric CODH subunit and two CooF subunits. The native molecular mass of CooF was estimated to be 29 kDa by analytical gel filtration, which lies between a monomer and dimer, so we cannot distinguish whether CODH is bound as two individual monomers or a dimer. Though, in principle, the gel filtration data is also consistent with a heterotrimeric CODH:CooF, the data described below are better rationalized by assigning CODH:CooF a tertrameric structure.

Metal analysis of CODH:CooF is also consistent with the presence of two CooF subunits in CODH:CooF. This interpretation takes into account the 8–9 Fe/CODH monomer previously calculated for multiple preparations of CODH, which is lower than the number of Fe atoms predicted by the crystal structure of *R. rubrum* CODH [29,32,36]. Assuming 16–18 Fe/CODH dimer, addition of two CooF subunits (7±2 Fe/monomer) would give 30–32 Fe/CODH:CooF complex, close to the experimental value of 28±2 Fe/CODH:CooF. The observed ratio of 7±2 Fe/CooF monomer is inconsistent with the experimental value obtained by Ensign and Ludden (4 Fe/CooF monomer). However, the extinction coefficients measured for A_{420} of CooF by Ensign and Ludden were 37 cm^{-1} mM^{-1} for oxidized CooF and 17 cm^{-1} mM^{-1} for reduced CooF. These values are most similar to previously reported extinction coefficients for 8-Fe ferreodxins [37]. EPR studies of CooF were also consistent with the assignment of CooF as an 8-Fe ferredoxin (see below).

The B and C-clusters signals of CODH are essentially insensitive to CooF complexation. Both the C-cluster (C_{red1}, C_{red2}) and B-cluster (B_{red}) signals observed for CODH:CooF are identical in *g* value to the signals reported for CODH and are generated under similar conditions. Also, no unique signature was identified that corresponded to a reduced form of the D-cluster (D_{red}). CODH:CooF has a lower spin concentration than would be expected based on the number of paramagnetic metal clusters in the complex (2 spins/tetramer expected for phenosafranin-treated CODH:CooF (0.2 spins/tetramer observed); 9 spins/tetramer expected for CO-treated CODH:CooF (6.5 spins/tetramer observed)). Low spin concentrations have been measured for the EPR spectra of *R. rubrum* CODH and *M. thermoacetica* ACS/CODH and have been attributed to spin state heterogeneity of the metal clusters of CODH [32,38,39].

Two features of the EPR spectra of the reduced forms of CODH:CooF distinguish it from the spectra of CODH. The first feature arises from direct comparison of the EPR spectra of CO-reduced CODH:CooF with the spectra of DTH-reduced CODH:CooF at 10 K. Under these conditions, the spectrum of DTH-reduced CODH:CooF integrates to a lower spin concentration and lacks the C_{red2} signal, which is only observed when the measurement is taken at 4.5 K. Unlike CODH:CooF, the EPR spectra of both CO-reduced CODH and DTH-reduced CODH have nearly equal spin concentrations and C_{red2} is observed for both spectra at 10 K. The difference in intensity was unexpected because both CO and DTH reduce the Fe–S clusters of CODH:CooF equally as measured by extinction coefficients for A_{420} (36 mM^{-1} cm^{-1}). Interestingly, the same reductant-dependent phenomenon is observed for CODH (β_2 homodimer) from *C. hydrogenoformans*, where EPR spectra (10 K, 10 mW power) are more intense for the CO-reduced CODH than DTH-reduced CODH [40]. Also, DTH-reduced CODH from *C. hydrogenoformans* lacks the C_{red2} signal at 10 K, which is observed for CO-reduced CODH. The differential effects of CO and DTH may arise because CODH:CooF spontaneously consumes DTH, leading to a more oxidized state of the protein as observed by EPR. Lindahl and coworkers have observed spontaneous consumption of DTH by ACS/CODH from *M. thermoacetica* [41]. A second explanation for the difference may be that the metal clusters of CODH have different relaxation properties when treated with CO or DTH. Ludden and co-workers have proposed that the metal clusters of CODH interact extensively, leading to the unusual spectra obtained for CODH [29].

The second feature that distinguishes the EPR spectra of CODH:CooF from CODH is the additional signal attributed to the Fe–S clusters of CooF. This signal is readily observed in CO-reduced CODH:CooF and DTH-reduced Ni-deficient CODH:CooF. As mentioned in the Results section, the spectrum of DTH-reduced CooF is characteristic of ferredoxins containing 2 $[Fe_4S_4]^{1+}$ clusters whose unpaired electrons have a strong exchange interaction. A survey of the literature revealed that the

DTH-reduced 8Fe Fix ferredoxin isolated from *Azotobacter vinelandii* has a nearly identical spectrum to DTH-reduced CooF [34]. This comparison, along with the spin concentration of CooF (2.0 spins/monomer) provides persuasive evidence that CooF contains 2 Fe_4S_4 clusters. EPR experiments with CooF confirm the results of Fe metal analysis and interpretation of the extinction coefficients for A_{420} of CooF, which also are consistent with an 8-Fe protein. This conclusion is in striking contrast to spectroscopic and crystallographic characterization of CooF homologs NarH, DmsB and the FdhN β-subunit, all of which contain 4 Fe–S clusters [42–44]. This conclusion also contradicts the assignment of 4 Fe_4S_4 clusters to CooF isolated as part of the CO-oxidizing/H_2 evolving complex of *C. hydrogenoformans*.

4.2. Low in vitro CO-dependent H_2 evolution may be due to loss of Fe–S clusters from CooF

As mentioned in the Introduction, rates of *in vitro* CO-dependent H_2 evolution by *R. rubrum* membranes are at least 10-fold lower than expected rates based on *in vivo* measurements. Also, this study has confirmed that rates of MV-dependent H_2 evolution are >10-fold higher than CO-dependent H_2 evolution by *R. rubrum* membranes. For the *C. hydrogenoformans* CO-oxidizing/H_2 evolving complex rates of CO-dependent H_2 evolution were higher than MV-dependent H_2 evolution for the membrane fraction as well as the purified complex [20]. These data led us to hypothesize that the CO-oxidizing H_2 evolving complex of *R. rubrum* was damaged during isolation, and comparison of *in vivo* and *in vitro* CO-dependent H_2 evolution confirmed that the activity loss occurred when the *R. rubrum* cells were lysed. Spectroscopic studies of CODH:CooF indicated that CooF contained only 2 Fe_4S_4 clusters, In contrast, the purified *C. hydrogenoformans* CO-oxidizing H_2 evolving complex has 4 Fe_4S_4 clusters in each CooF subunit and is fully competent for CO-dependent H_2 evolution. We propose that two of the Fe–S clusters of CooF are labile and dissociate from the protein during cell lysis. These Fe–S clusters may be critical for efficient CO-dependent H_2 evolution and cause the lowered activities observed for *in vitro* CO-dependent H_2 evolution by *R. rubrum*. The lability of cysteine-ligated Fe–S clusters has recently been documented for NapF, an Fe–S protein involved in the biosynthesis of periplasmic nitrate reductase [45]. An alternative possibility is that *R. rubrum* CooF contains two Fe_4S_4 *in vivo*, and the loss of activity results from simply disrupting the CO oxidizing/H_2 evolving complex of *R. rubrum*. This result would suggest a fundamental difference between the CO-oxidizing/H_2 evolving complexes in *R. rubrum* compared to *C. hydrogenoformans*.

4.3. Membrane-bound R. rubrum CO-induced hydrogenase is fully functional for H_2 evolution

In most uptake hydrogenases, only CooH and CooL are required to observe MV-dependent H_2 evolution. However, evidence suggests that the *R. rubrum* CO-induced hydrogenase requires the additional subunits (CooMKXU) to catalyze both CO-dependent and MV-dependent H_2 evolution. CO-dependent and MV-dependent H_2 evolution by the CO-induced hydrogenase are inhibited by *N,N′*-dicyclohexyldiimide (DCCD), an inhibitor of proton translocation in Complex 1, implying that H_2 evolution and proton translocation are coupled in the hydrogenase [9]. Since DCCD modifies a hydrophobic subunit of Complex 1, the hydrophobic subunits of the CO-induced hydrogenase, CooM or CooK, are the probable targets for DCCD modification [46]. Therefore, the hydrophobic subunits of the CO-induced hydrogenase seem to be required for H_2 evolution with CO and MV as electron donors. A second line of evidence arises from recent site-directed mutagenesis studies of the *M. barkeri* Ech hydrogenase, a homolog of the CO-induced hydrogenase, reported by Hedderich and co-workers [47]. Variation of cysteine residues of EchF, a hydrophilic Fe–S protein homologous to CooX, caused nearly identical decreases in H_2-dependent reduction of *M. barkeri* ferredoxin, the natural electron acceptor for the Ech hydrogenase, and BV, when compared to the wild-type Ech hydrogenase. The authors proposed that the Ech hydrogenase has an identical pathway for both natural and artificial electron acceptors to receive electrons from H_2 oxidation. Taken together, the observation of DCCD inhibition of the CO-induced hydrogenase and the site-directed mutagenesis studies of the Ech hydrogenase suggest that damage to the CO-induced hydrogenase would result in substantial loss of CO-dependent *and* MV-dependent H_2 evolution activities in cell extracts compared to whole cells.

4.4. CODH:CooF is required for optimal activity of CO-induced hydrogenase

Development of new assay for CODH:CooF led to the unexpected observation that the CO-induced hydrogenase from UR282 membranes was less active than the CO-induced hydrogenase from UR2 membranes. Comparison with UR294, an *R. rubrum* mutant that expresses CODH:CooF but does not express CooCTJ, indicated that the absence of the genes products involved in Ni processing into CODH had no effect on the activity of the CO-induced hydrogenase. Therefore, the presence of CODH:CooF appears to affect the stability of the CO-induced hydrogenase. However, Ludden and Ensign observed that the MV-dependent H_2 evolution activity of the CO-induced hydrogenase was minimally affected (>70% recovery) by repeated detergent washing of UR2 membranes which removed CODH:CooF, suggesting that the CO-induced hydrogenase is stable *in vitro* [18]. An alternative explanation for this low observed activity is that the CO-induced hydrogenase requires CODH:CooF to form properly *in vivo*, resulting in the lower activities observed *in vitro*. Future studies may focus on detailed characterization of the additional subunits of the CO-induced hydrogenase to understand their role in CO-dependent H_2 evolution.

Acknowledgements

We thank Professor Gary Roberts and Dr. Robert Kerby of the University of Wisconsin-Madison for providing the *R.*

rubrum mutant strains. We thank Dr. Simon George and Professor Steve Cramer of Lawrence Berkeley National Laboratory for the use of their EPR spectrometer.

Work described here was supported by grant DE-FG02-87ER13691 (DOE Basic Energy Sciences program) to P. W. L.

References

[1] D.B. Levin, L. Pitt, M. Love, Biohydrogen production: prospects and limitations to practical application, Int. J. Hydrogen Energy 29 (2004) 173–185.

[2] D. Das, T.N. Veziroglu, Hydrogen production by biological processes: a survey of literature, Int. J. Hydrogen Energy 26 (2001) 13–28.

[3] P.C. Hallenbeck, J.R. Benemann, Biological hydrogen production; fundamentals and limiting processes, Int. J. Hydrogen Energy 27 (2002) 1185–1193.

[4] P.C. Maness, P.F. Weaver, Evidence for three distinct hydrogenase activities in *Rhodospirillum rubrum*, Appl. Microbiol. Biotechnol. 57 (2001) 751–756.

[5] R.L. Kerby, P.W. Ludden, G.P. Roberts, Carbon monoxide-dependent growth of *Rhodospirillum rubrum*, J. Bacteriol. 177 (1995) 2241–2244.

[6] R.L. Kerby, P.W. Ludden, G.P. Roberts, In vivo nickel insertion into the carbon monoxide dehydrogenase of *Rhodospirillum rubrum*: molecular and physiological characterization of CooCTJ, J. Bacteriol. 179 (1997) 2259–2266.

[7] D. Shelver, R.L. Kerby, Y.P. He, G.P. Roberts, Carbon monoxide-induced activation of gene expression in *Rhodospirillum rubrum* requires the product of CooA, a member of the cyclic-AMP receptor protein family of transcriptional regulators, J. Bacteriol. 177 (1995) 2157–2163.

[8] R.L. Kerby, S.S. Hong, S.A. Ensign, L.J. Coppoc, P.W. Ludden, G.P. Roberts, Genetic and physiological characterization of the *Rhodospirillum rubrum* carbon monoxide dehydrogenase system, J. Bacteriol. 174 (1992) 5284–5294.

[9] J.D. Fox, Y.P. He, D. Shelver, G.P. Roberts, P.W. Ludden, Characterization of the region encoding the CO-induced hydrogenase of *Rhodospirillum rubrum*, J. Bacteriol. 178 (1996) 6200–6208.

[10] D. Bonam, P.W. Ludden, Purification and characterization of carbon monoxide dehydrogenase, a nickel, zinc, iron–sulfur protein, from *Rhodospirillum rubrum*, J. Biol. Chem. 262 (1987) 2980–2987.

[11] C.L. Drennan, J.Y. Heo, M.D. Sintchak, E. Schreiter, P.W. Ludden, Life on carbon monoxide: X-ray structure of *Rhodospirillum rubrum* Ni–Fe–S carbon monoxide dehydrogenase, Proc. Nat. Acad. Sci. U. S. A. 98 (2001) 11973–11978.

[12] C. Darnault, A. Volbeda, E.J. Kim, P. Legrand, X. Vernede, P.A. Lindahl, J.C. Fontecilla-Camps, Ni–Zn–[Fe_4S_4] and Ni–Ni–[Fe_4S_4] clusters in closed and open subunits of acetyl-CoA synthase/carbon monoxide dehydrogenase, Nat. Struct. Biol. 10 (2003) 271–279.

[13] H. Dobbek, V. Svetlitchnyi, L. Gremer, R. Huber, O. Meyer, Crystal structure of a carbon monoxide dehydrogenase reveals a [Ni–4Fe–5S] cluster, Science 293 (2001) 1281–1285.

[14] R. Hedderich, Energy-converting [NiFe] hydrogenases from archaea and extremophiles: ancestors of complex I, J. Bioenerg. Biomem. 36 (2004) 65–75.

[15] J.D. Fox, R.L. Kerby, G.P. Roberts, P.W. Ludden, Characterization of the CO-induced, CO-tolerant hydrogenase from *Rhodospirillum rubrum* and the gene encoding the large subunit of the enzyme, J. Bacteriol. 178 (1996) 1515–1524.

[16] P.C. Maness, J. Huang, S. Smolinski, V. Tek, G. Vanzin, Energy generation from the CO oxidation-hydrogen production pathway in *Rubrivivax gelatinosus*, App. Environ. Microbiol. 71 (2005) 2870–2874.

[17] R. Sapra, K. Bagramyan, M.W.W. Adams, A simple energy-conserving system: proton reduction coupled to proton translocation, Proc. Natl. Acad. Sci. U. S. A. 100 (2003) 7545–7550.

[18] S.A. Ensign, P.W. Ludden, Characterization of the CO oxidation/H_2 evolution system of *Rhodospirillum rubrum*—role of a 22-KDa iron–sulfur protein in mediating electron transfer between carbon monoxide dehydrogenase and hydrogenase, J. Biol. Chem. 266 (1991) 18395–18403.

[19] K.T. Klasson, K.M.O. Lundback, E.C. Clausen, J.L. Gaddy, Kinetics of light limited growth and biological hydrogen production from carbon monoxide and water by *Rhodospirillum rubrum*, J. Biotechnol. 29 (1993) 177–188.

[20] B. Soboh, D. Linder, R. Hedderich, Purification and catalytic properties of a CO-oxidizing:H_2-evolving enzyme complex from *Carboxydothermus hydrogenoformans*, Eur. J. Biochem. 269 (2002) 5712–5721.

[21] D. Bonam, S.A. Murrell, P.W. Ludden, Carbon monoxide dehydrogenase from *Rhodospirillum rubrum*, J. Bacteriol. 159 (1984) 693–699.

[22] S.A. Ensign, M.R. Hyman, P.W. Ludden, Nickel-specific, slow-binding inhibition of carbon monoxide dehydrogenase from *Rhodospirillum rubrum* by cyanide, Biochemistry 28 (1989) 4973–4979.

[23] S.A. Ensign, M.J. Campbell, P.W. Ludden, Activation of the nickel-deficient carbon monoxide dehydrogenase from *Rhodospirillum rubrum* —Kinetic characterization and reductant requirement, Biochemistry 29 (1990) 2162–2168.

[24] P.W. Ludden, R.H. Burris, Activating factor for iron protein of nitrogenase from *Rhodospirillum rubrum*, Science 194 (1976) 424–426.

[25] U.K. Laemmli, Cleavage of structural proteins during the assembly of the head of bacteriophage T4, Nature 227 (1970) 680–685.

[26] M.S. Blake, K.H. Johnston, G.J. Russell-Jones, E.C. Gotschlich, A rapid, sensitive method for detection of alkaline-phosphatase conjugated anti-antibody on western blots, Anal. Biochem. 136 (1984) 175–179.

[27] P.K. Smith, R.I. Krohn, G.T. Hermanson, A.K. Mallia, F.H. Gartner, M.D. Provenzano, E.K. Fujimoto, N.M. Goeke, B.J. Olson, D.C. Klenk, Measurement of protein using bicinchoninic acid, Anal. Biochem. 150 (1985) 76–85.

[28] N.J. Spangler, P.A. Lindahl, V. Bandarian, P.W. Ludden, Spectroelectrochemical characterization of the metal centers in carbon monoxide dehydrogenase (CODH) and nickel-deficient CODH from *Rhodospirillum rubrum*, J. Biol. Chem. 271 (1996) 7973–7977.

[29] J. Heo, C.R. Staples, J. Telser, P.W. Ludden, *Rhodospirillum rubrum* CO-dehydrogenase. Part 2. Spectroscopic investigation and assignment of spin–spin coupling signals, J. Am. Chem. Soc. 121 (1999) 11045–11057.

[30] E.T. Smith, S.A. Ensign, P.W. Ludden, B.A. Feinberg, Direct electrochemical studies of hydrogenase and CO dehydrogenase, Biochem. J. 285 (1992) 181–185.

[31] J.L. Craft, P.W. Ludden, T.C. Brunold, Spectroscopic studies of nickel-deficient carbon monoxide dehydrogenase from *Rhodospirillum rubrum*: nature of the iron–sulfur clusters, Biochemistry 41 (2002) 1681–1688.

[32] Z.G. Hu, N.J. Spangler, M.E. Anderson, J.Q. Xia, P.W. Ludden, P.A. Lindahl, E. Munch, Nature of the C-cluster in Ni-containing carbon monoxide dehydrogenases, J. Am. Chem. Soc. 118 (1996) 830–845.

[33] R. Mathews, S. Charlton, R.H. Sands, G. Palmer, Nature of spin coupling between iron–sulfur clusters in 8-Fe ferredoxins, J. Biol. Chem. 249 (1974) 4326–4328.

[34] B. Reyntjens, D.R. Jollie, P.J. Stephens, H.S. GaoSheridan, B.K. Burgess, Purification and characterization of a FixABCX-linked 2[4Fe–4S] ferredoxin from *Azotobacter vinelandii*, J. Biol. Inorg. Chem. 2 (1997) 595–602.

[35] H.G. Koch, M. Kern, J.H. Klemme, Reinvestigation of regulation of biosynthesis and subunit composition of nickel-dependent Hup-hydrogenase of *Rhodospirillum rubrum*, FEMS Microbiol. Lett. 91 (1992) 193–197.

[36] J.Y. Heo, C.R. Staples, C.M. Halbleib, P.W. Ludden, Evidence for a ligand CO that is required for catalytic activity of CO dehydrogenase from *Rhodospirillum rubrum*, Biochemistry 39 (2000) 7956–7963.

[37] K.R. Carter, J. Rawlings, W.H. Orme-Johnson, R.R. Becker, H.J. Evans, Purification and characterization of a ferredoxin from *Rhizobium japonicum* bacteroids, J. Biol. Chem. 255 (1980) 4213–4223.

[38] D.M. Fraser, P.A. Lindahl, Stoichiometric CO reductive titrations of acetyl-CoA synthase (carbon monoxide dehydrogenase) from *Clostridium thermoaceticum*, Biochemistry 38 (1999) 15697–15705.

[39] P.A. Lindahl, The Ni-containing carbon monoxide dehydrogenase family: light at the end of the tunnel? Biochemistry 41 (2002) 2097–2105.

[40] V. Svetlitchnyi, C. Peschel, G. Acker, O. Meyer, Two membrane-

associated NiFeS-carbon monoxide dehydrogenases from the anaerobic carbon monoxide-utilizing eubacterium *Carboxydothermus hydrogenoformans*, J. Bacteriol. 183 (2001) 5134–5144.

[41] J. Feng, P.A. Lindahl, Effect of sodium sulfide on Ni-containing carbon monoxide dehydrogenases, J. Am. Chem. Soc. 126 (2004) 9094–9100.

[42] M. Jormakka, S. Tornroth, B. Byrne, S. Iwata, Molecular basis of proton motive force generation: structure of formate dehydrogenase-N, Science 295 (2002) 1863–1868.

[43] M. Jormakka, D. Richardson, B. Byrne, S. Iwata, Architecture of NarGH reveals a structural classification of Mo-bisMGD enzymes, Structure 12 (2004) 95–104.

[44] J.H. Weiner, R.A. Rothery, D. Sambasivarao, C.A. Trieber, Molecular analysis of dimethylsulfoxide reductase—a complex iron–sulfur molybdoenzyme of *Escherichia coli*, Biochim. Biophys. Acta 1102 (1992) 1–18.

[45] M.F. Olmo-Mira, M. Gavira, D.J. Richardson, F. Castillo, C. Moreno-Vivian, M.D. Roldan, NapF is a cytoplasmic iron–sulfur protein required for Fe–S cluster assembly in the periplasmic nitrate reductase, J. Biol. Chem. 279 (2004) 49727–49735.

[46] T. Yagi, Y. Hatefi, Identification of the dicyclohexylcarbodiimide-binding subunit of NADH-Ubiquinone oxidoreductase (Complex I), J. Biol. Chem. 263 (1988) 16150–16155.

[47] L. Forzi, J. Koch, A.M. Guss, C.G. Radosevich, W.W. Metcalf, R. Hedderich, Assignment of the [4Fe–4S] clusters of Ech hydrogenase from *Methanosarcina barkeri* to individual subunits via the characterization of site-directed mutants, FEBS J. 272 (2005) 4741–4753.